Talanta xxx (xxxx) xxxx

Contents lists available at ScienceDirect

Talanta

journal homepage: www.elsevier.com/locate/talanta

Electrochemical detection of microRNAs based on AuNPs/CNNS nanocomposite with Duplex-specific nuclease assisted target recycling to improve the sensitivity

Xiangyu Ma[a], Haoran Xu[a], Kun Qian[a], Martha Kandawa-Schulz[b], Weimin Miao[c], Yihong Wang[a,*]

[a] School of Chemistry and Chemical Engineering, Southeast University, Nanjing, 211189, PR China
[b] Department of Chemistry and Biochemistry, University of Namibia, Windhoek, Namibia
[c] Jiangsu Meizhong Medical Technology Co., Ltd., Nantong, China

ARTICLE INFO

Keywords:
Au nanoparticles
Carbon nitride nano sheet
Duplex-specific nuclease
Electrochemical biosensor
microRNAs

ABSTRACT

MicroRNAs (miRNAs) are important biomarkers in early diagnosis of disease. In this work, we developed a simple and effective electrochemical biosensor based on Au nanoparticles (AuNPs)/Carbon nitride nanosheet (CNNS) nanocomposite for the miRNAs detection. Duplex-specific nuclease (DSN) and hairpin structure probe were utilized to improve the sensitivity and selectivity respectively. In the presence of miRNA-21, the signal molecule could be released from the surface of the electrode and decrease the current peak in square wave voltammetry (SWV) test. Under the optimal conditions, the reported biosensor showed that the detection range of miRNA-21 is from 10 fM to 1 nM and detection limit is as low as 2.9 fM. Furthermore, the detection of miRNA-21 added in serum samples indicates the developed biosensor with good selectivity, stability and reproducibility which verify its potential to be used in the early diagnosis of diseases.

1. Introduction

MicroRNAs(miRNAs) are a class of non-coding single-stranded RNA molecules of approximately 18–24 nucleotides in length encoded by endogenous genes, which can regulate cell proliferation, differentiation and apoptosis [1,2]. Recent studies have shown that miRNAs recognize and bind to a target molecule in a base-complemented form, causing their expression to rise or fall, thereby regulating tumorigenesis [3]. In a word, abnormal expression of miRNAs is relevant with various cancer, gene disorder and immunocompromised [4]. Therefore, miRNAs are an emerging tumor biomarker for early diagnosis and prognostic, and their sensitive and selective analysis are beneficial for researchers to understand the miRNAs associated cancer [5]. However, it is still a huge challenging to detect miRNAs for their intrinsic properties including short length, low enrichment and sequence homology between family members [6,7]. There are several commonly methods for miRNAs analysis, for instance, reverse transcription-polymerase chain reaction (RT-PCR) [8], Northern blotting [9], and microarray technology [10]. Nevertheless, these methods are usually time-consuming, high cost, expensive equipment requirement, low sensitivity and false positive signal.

Recent years, a large number of advanced approaches have been applied to detect and quantify miRNAs, such as colorimetry [11], surface plasmon resonance (SPR) [12,13], fluorescence [14,15], electrogenerated chemiluminescence (ECL) [16,17], photoelectrochemical (PEC) [18] and electrochemistry [19]. While electrochemical methods have drawn great attention due to their intrinsic advantages, high sensitivity, high accuracy, wide measuring range and low equipment requirements [20,21]. But, electrochemical methods usually require a stable substrate to immobilize the probe molecule and guarantee the high reproducibility of detection. Gold electrode was often used as a working electrode for thiol-modified nucleic acid molecule could be immobilized on the surface of the gold electrode through Au–S bond [22,23]. The sensitivity and conductivity were limited by the gold electrode.

While nanotechnology was always combined with electrochemical methods to develop ultrasensitive electrochemical biosensors with small sample consume, good specificity, a wide detection range, good reproducibility, small size and low detection limits [24]. Nanomaterials are utilized in the construction of electrochemical biosensors due to their unique physicochemical properties, including excellent conductivity, large surface area, good stability and biocompatibility [25]. To date, graphene [26], carbon nanotube [27], C_3N_4 [28], metal oxides [29], Au nanoparticles (AuNPs) [30] and so on have been adopted in a

* Corresponding author.
E-mail address: yihongwang@seu.edu.cn (Y. Wang).

https://doi.org/10.1016/j.talanta.2019.120441
Received 8 July 2019; Received in revised form 17 September 2019; Accepted 3 October 2019

number of studies to create electrochemical biosensors with excellent performance. Among them, carbon nitride (CN) is an emerging two-dimensional carbon material, graphite-like CN (gCN) has drawn great attention in the application of electrocatalysis, photocatalysis and biosensors [31] ascribed to its inherent characteristic, such as high stability, ease of synthesis and rich raw materials [32]. However, the application in electrochemical detection of gCN is limited for its structure with hardly functional group, and gCN is difficult to be functionalized. While AuNPs have been widely used in many fields [33,34] for their good biocompatibility, simple synthetic operation, precisely controlled particle physicochemical properties, and unique tunable electronic properties [35]. Composite of two-dimensional material and AuNPs is a good substrate material for electrochemical biosensor applications. Qian et al. [36] prepared Au/g-C_3N_4 composite through protonation, adsorption and reduction for enhanced photocatalytic hydrogen evolution. Feng et al. [37] reported on highly sensitive and selective detection of triclosan based on g–C_3N_4–AuNPs, and the composite was prepared through electrodeposition. However, the surface of these modified electrodes are hard to control and the AuNPs size is not uniformly, which could deteriorate the sensitivity and reduce the repeatability of the constructed biosensor.

In our work, we developed a simple and highly sensitive electrochemical biosensor based on a composite of CN nanosheet (CNNS) and size-controlled AuNPs. Thiol modified aptamer capture target DNA (cDNA) was immobilized onto AuNPs through Au–S bond and miRNA was captured by cDNA according to base pairing principle. In addition, Methylene blue (MB) modified on the 3' of cDNA was utilized as an electrochemical signal. Besides, Duplex-Specific Nuclease (DSN) was used to amplify the signal difference of the electrochemical biosensor. In the absence of miRNA, the square wave voltammetry (SWV) signal of MB is very strong. In contrast, the SWV signal of MB is weaker in the presence of miRNA for the DSN can selectively cleave cDNA of the cDNA-miRNA hybrid and release the miRNA repeatedly. $_{\Delta}I$ of current peak I_{pa} in the presence of miRNA and current peak I_{pb} in the absence of miRNA is related to the concentration of miRNA. Therefore, taking advantage of base pair principle and DSN which makes the target detected specifically. The developed electrochemical biosensor exhibits high selectivity, reproducibility and sensitivity for the detection of miRNA. In real sample detection, the biosensor shows excellent performance as well.

2. Experimental

2.1. Chemicals and reagents

$HAuCl_4$, Dicyandiamide, and Polyethyleneimine (PEI) were purchased from Aladdin Reagent Company (Shanghai, China). Tris(2-carboxyethyl)phosphine (TCEP) were purchased from Sinopharm Chemical Reagent Co., Ltd. Human serum samples (H4522) were purchased from Sigma-Aldrich. DSN, starting solution (pH = 8.0, 500 mM Tris-HCl, 50 mM $MgCl_2$ and 10 mM DTT) and stop solution (10 mM EDTA) was provided by Newborn Biotechnology Co., Ltd (Shenzhen, China). All other reagents used are of analytical grade. In this work, supporting electrolyte was 10 mM phosphate buffered saline (PBS pH = 7.0). All aqueous solutions were prepared with ultrapure water (18.2 MΩ cm) utilizing an Aquapro water purification system. In addition, a typical biomarker of breast cancer miRNA-21 was used as a representative miRNA and all oligonucleotides were obtained from Sangon Biotech Co., Ltd (Shanghai, China). The sequences of these oligonucleotides were shown in Table S1 and the cDNA was designed according to the principle that DSN could selectively cleave DNA at least continuous 10 base pairs (bp) in dsDNA or 15 bp in DNA/RNA hybrid [38–40].

2.2. Apparatus and measurements

All electrochemical experiments were conducted in a conventional three electrodes system (a 3.0 mm diameter glassy carbon electrode (GCE), a platinum wire electrode and a saturated calomel electrode (SCE) as working electrode, counter electrode and reference electrode respectively) with a CHI660E electrochemical workstation (Shanghai Chenhua Instruments, China). The electrochemical techniques employed including cyclic voltammetry (CV), AC impedance (EIS) and SWV. Transmission electron microscopy (TEM) test utilized a Hitachi H-800 microscope (Japan).

2.3. Preparation of AuNPs and CNNS modified electrode (AuNPs/CNNS/GCE)

In order to prepare the CNNS, bulk CN was first prepared. Bulk CN was prepared according to Zhou's method [41]. Briefly, dicyandiamide was heated at 550 °C for 4 h with a ramp rate of 3 °C min^{-1} in air atmosphere. Then the cooled product was ground into fine powder using agate mortar. Next, 10 mg bulk CN was added to 10 ml ultrapure water and ultrasonically dissolved for approximately 16 h. Finally, the mixture was centrifuged for 10 min at 2400 g and collect the supernatant. The concentration of the CNNS is calculated by the weighing method as 15 mg mL^{-1}. Besides, PEI modified AuNPs was synthesized according to Kim's method [42], and details were shown in support information.

Then AuNPs/CNNS was synthesized by simply mixing the positively charged PEI modified AuNPs and negatively charged CNNS [43] in a certain ratio through electrostatic adsorption interaction. Then the mixture was ultrasonically oscillated for 10 min to obtain a homogeneous solution and stored at 4 °C for use.

2.4. Fabrication of the biosensor for detecting miRNA

Before fabricate the biosensor, bare GCE was polished with 0.05 μm and 0.3 μm alumina-water slurries on the surface of clammy to obtain a mirror-like surface. Then, the GCE was washed by ultrasonic oscillation using distilled deionized water to remove residual alumina particles and dry under nitrogen flow. Next, 10 μl AuNPs/CNNS composite was dropped onto the surface of GCE and dried naturally at room temperature. Afterwards, the mixture of 5 μl of cDNA treated with TCEP, 2 μl of DSN and 5 μl of miRNA-21 in 10 fM, 100 fM, 1 pM, 10 pM, 100 pM and 1 nM respectively were incubated at 65 °C for 1.5 h (starting solution and stop solution were used to control the reaction). After that, incubating solution was dropped onto the surface of AuNPs/CNNS modified GCE and dried naturally at room temperature. Finally, PBS buffer was used to wash the GCE to remove non-specific adsorption, the proposed miRNA biosensor was constructed as illustrated in Fig. 1.

The peak current (Ip) of the constructed biosensor could be affected by several factors, as property of CNNS (including concentration, number of layers), ratio of AuNPs/CNNS, incubation time of cDNA-miRNA-21 and DSN, and the concentration of cDNA. To optimize the performance of the proposed biosensor, the factors mentioned above was explored to get optimal condition.

3. Results and discussion

3.1. Characterization of AuNPs/CNNS

To observe the morphologies of the assembled nanomaterial, composite AuNPs/CNNS was characterized by TEM. As shown in Fig. S1, PEI capped positively charged AuNPs were uniformly dispersed on the surface of CNNS [44]. Besides, high-resolution TEM image (Fig. 2) of composite AuNPs/CNNS shows that AuNPs were the same size and CNNS were very thin, likely to be few-layered. It indicates that the positively charged AuNPs and negatively charged CNNS were assembled successfully and the nanocomposite were obtained.

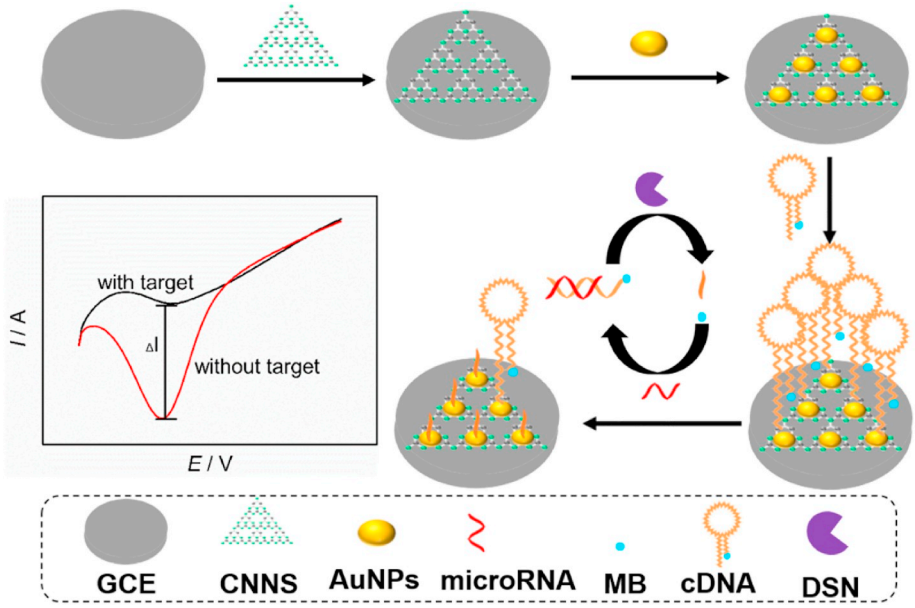

Fig. 1. Schematic representation of the fabrication of the electrochemical biosensor and the detection principle.

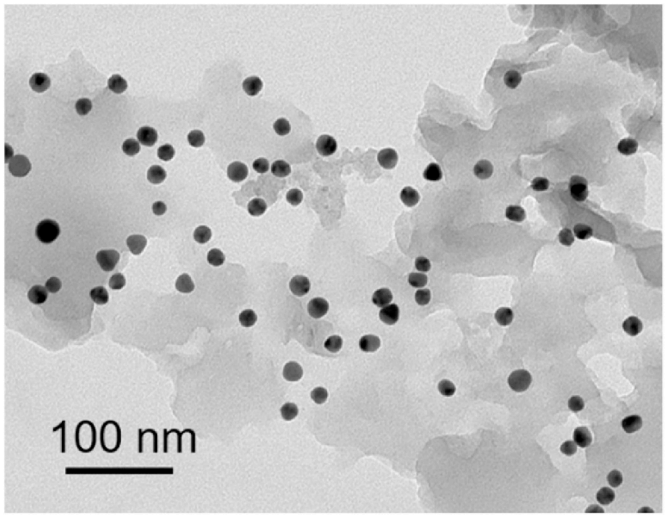

Fig. 2. High resolution image of AuNPs/CNNS.

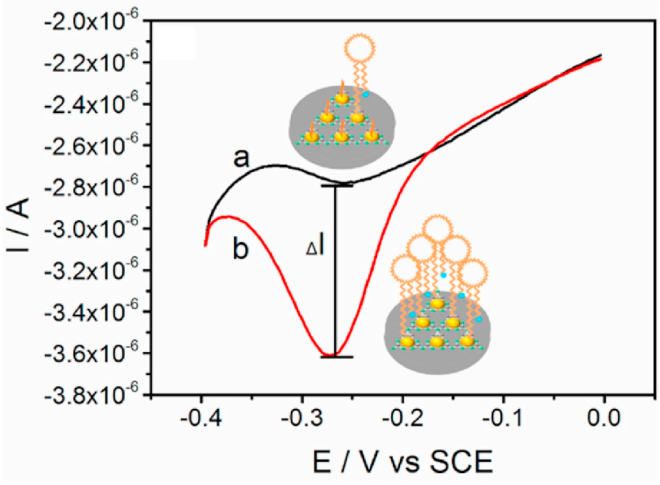

Fig. 3. SWV of proposed electrochemical biosensors in the (a) presence and (b) absence of miRNA-21.

3.2. Feasibility of the miRNA-detection strategy

To confirm the feasibility of the proposed electrochemical biosensor for miRNA detection, the Ip of SWV in the presence and absence of target were compared. Fig. 3 shows the SWV curves of different configurations on the AuNPs/CNNS/GCE surface. In the absence of target miRNA-21, DSN could not work on the cDNA according to the cutting principle [38] and the SWV signal generated by the reduction reaction of MB was stronger (curve b). When in the presence of miRNA-21, MB modified cDNA could hybrid with miRNA-21 and DSN could work on cDNA-miRNA-21 to release MB and miRNA-21 [45–47]. Then, the later retargeted to cDNA and cDNA was cleaved constantly. As a result, few signal molecule remained on the surface of the electrode and the SWV signal was significantly decreased in the presence of the target (curve a). In this period, miRNA acted as a catalytic role and enhanced the difference of the electrical signal. These results demonstrate that the strategy used could enhance the sensitivity of electrochemical detection for miRNA-21.

3.3. CV and EIS of the proposed biosensor

In order to further explore the feasibility of the proposed biosensor, CV and EIS were performed to verify the stepwise assembly processes of the modified electrode [48]. Fig. 4A was cyclic voltammograms of different assembly layer in $[Fe(CN)_6]^{3-/4-}$. A couple of reversible redox peaks of $[Fe(CN)_6]^{3-/4-}$ for bare GCE (curve a) were observed. After CNNS was modified onto the GCE, the Ip of the electrode decreased (curve b) for CNNS increased surface resistance and slow down the transmission of electrons. When AuNPs were located onto CNNS/GCE, the Ip of the electrode increased (curve c) due to the excellent conductivity of AuNPs. The attachment of cDNA (curve d) to AuNPs/CNNS/GCE decreased the Ip and increased the peak-potential separation, which indicates that cDNA was modified successfully through Au–S bond. As the miRNA hybrid with cDNA (curve e), the Ip of the electrode decreased remarkably because of the poor conductivity of miRNA or stronger electrostatic repulsion between negatively charged miRNA-DNA and $[Fe(CN)_6]^{3-/4-}$. Then the redox Ip of the $[Fe(CN)_6]^{3-/4-}$ on the DSN treated cDNA-miRNA modified electrode became lower

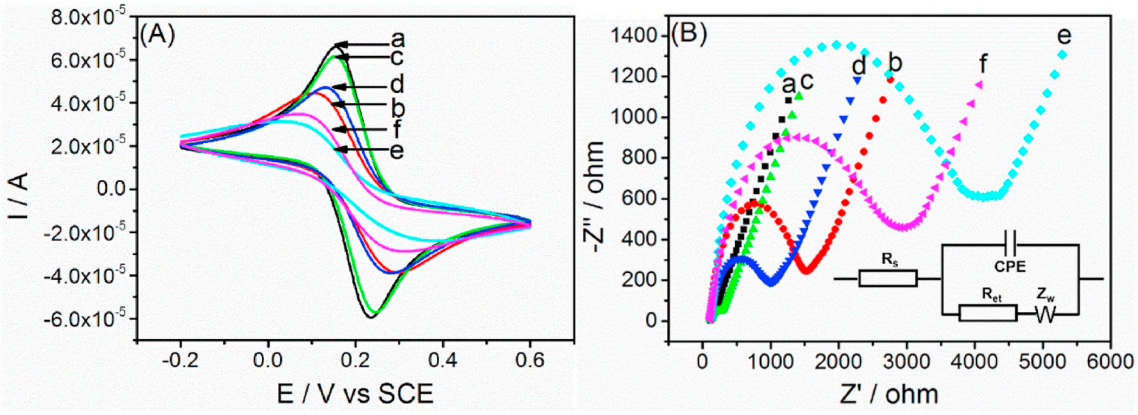

Fig. 4. (A) Cyclic voltammograms and (B) EIS Nyquist plots (The inset is the equivalent circuit of the Nyquist plots) of different steps in the fabrication of the electrode (a) bare GCE, (b) CNNS/GCE, (c) AuNPs/CNNS/GCE, (d) cDNA/AuNPs/CNNS/GCE, (e) miRNA-21-cDNA/AuNPs/CNNS/GCE, (f) DSN-miRNA-21-cDNA/AuNPs/CNNS/GCE. Experiments were conducted in 5.0 mM $Fe(CN)_6^{4-/3-}$ containing 0.1 M KCl at a scan rate of 100 mV s^{-1} of CV and the EIS frequency range is from 0.1 Hz to 100 kHz at 250 mV with amplitude of 5 mV.

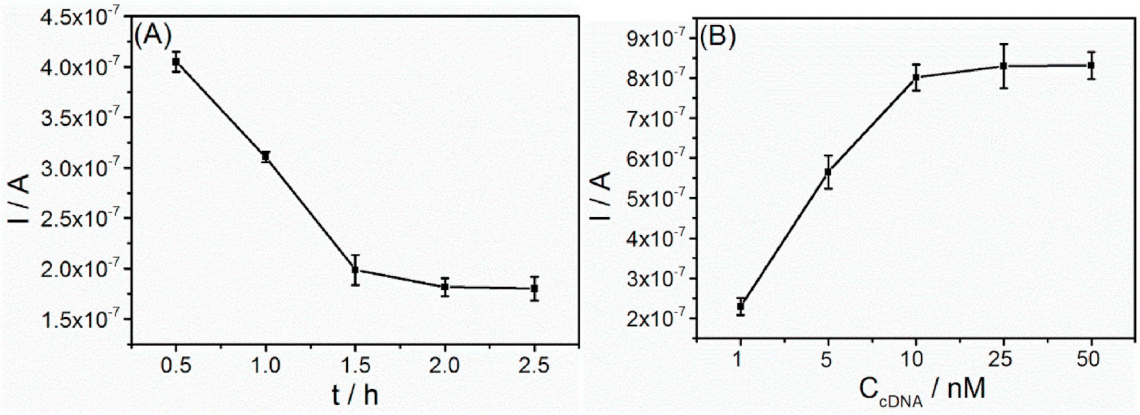

Fig. 5. The optional condition of (A) incubation time of cDNA-miRNA-21 and DSN, (B) cDNA concentration. SWV experiments were conducted in 0.01 M PBS (pH = 7.0) at a scan rate of 25 mV s^{-1}. Error bars = RSD (n = 5).

obviously suggesting that the reaction of DSN and cDNA-miRNA happened. All above mean that the assembly of the working electrode is successfully.

EIS has the same similar results with cyclic voltammograms. All the impedance containing solution resistance, electro-transfer resistance (R_{et}) can be calculated according to the Nyquist-plot [49]. As shown in Fig. 4B, all the solution resistance were similar. Except the electrode modified with AuNPs and DSN improved the conductivity of the electrode, the other modification increased the impedance of the electrode. These suggest that the construction of working electrode is very successful as well.

3.4. Optimization of the detection conditions

As shown in Fig. 5A, cDNA-miRNA-21 and DSN was incubated at varying incubation periods from 0.5 to 2.5 h. The results show that the Ip decreased rapidly from 0.5 to 1.5 h. After 1.5 h, the Ip decreased slowly, which indicating most MB signal molecules were removed. According to the principle of the proposed electrochemical biosensor, SWV signal needs to be as large as possible when the target did not exist. Based on this, different concentrations of cDNA were examined to get higher Ip, with the result in Fig. 5B showing that as the concentration of cDNA increased, the Ip became large rapidly until the cDNA concentration reached 10 nM. It should be that the cDNA was located onto the modified electrode by Au–S bond, and the quantity of AuNPs was determined and the amount of the cDNA could be immobilized with maximum. As a result, the optimized incubation time was 1.5 h, the optimized concentration of cDNA adopted for the biosensor was 10 nM.

3.5. Sensitivity of the miRNA biosensor

The performance of the proposed electrochemical biosensor in response to different concentrations of miRNA was investigated under the optimal experimental conditions. As shown in Fig. 6A, the SWV Ip decreased gradually with the increasing concentration of miRNA-21 from 10 fM to 1 nM. Simultaneously, the $_{\Delta}$Ip became larger gradually. A corresponding linear relationship was obtained between the $_{\Delta}$Ip and the logarithm of miRNA-21 concentration in the range from 10 fM to 1 nM (Fig. 6B), and the corresponding linear correlation equation is $_{\Delta}$Ip (μA) = 1.401 + 0.1058logC (R^2 = 0.9968), where $_{\Delta}$Ip is the Ip reduction ($_{\Delta}$Ip = Ipa - Ipb, where Ipa is the SWV current of the biosensor in the absence of miRNA-21 and Ipb is the SWV current of the biosensor in the presence of different concentration miRNA-21) and C is the concentration of miRNA-21. The limit of detection was easily calculated to be 2.9 fM (S/N = 3). As shown in Table 1, compared with previous studies, our limit of detection (LOD) is at a lower level. Even though the similar method was utilized in Xiao's work, lower LOD was obtained in our work for the weak adsorption capacity of MoS_2 and nucleic acid [15]. The successful construction of the sensor should be owing to the high surface area of CNNS, high conductivity of AuNPs/CNNS and signal difference amplification induced by the highly effective of DSN.

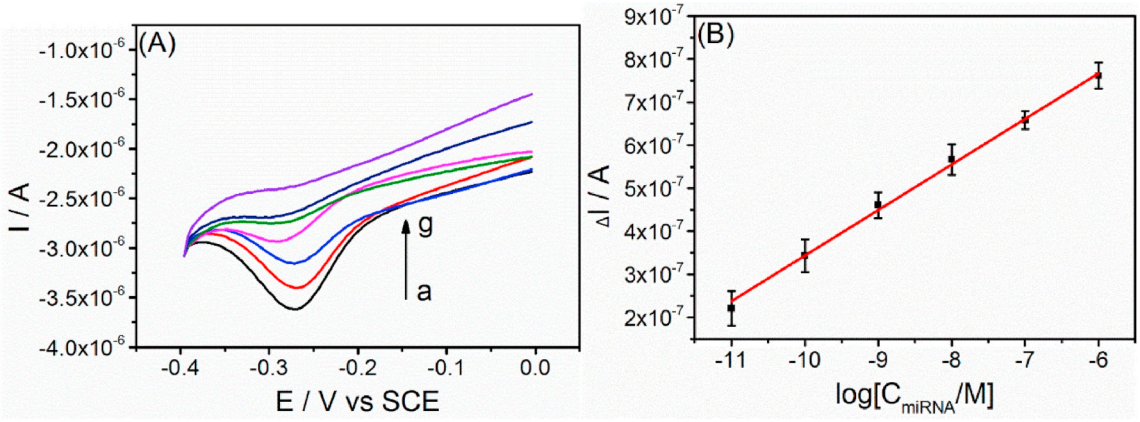

Fig. 6. (A) SWV responses to DSN/miRNA-21/cDNA/AuNPs/CNNS/GCE after incubating with different concentrations of miRNA-21 from (a) to (g): 0 M, 10 fM, 100 fM, 1 pM, 10 pM, 100 pM, 1 nM in 0.01 M PBS (pH = 7.0). (B) Standard curve of linear relationship between $_{\Delta}$I and logarithmic miRNA-21 concentration. Error bars = RSD (n = 5).

Table 1
Comparison with different biosensor for detection of nucleic acids.

Method	Analyte	signal amplification	Linear range	LOD	ref
ECL	miRNA-21	DSN	10 fM to 100 pM	5.4 fM	[17]
ICP-MS	miRNA-141	DSN	0 to 200 fM	58 fM	[51]
Fluorescence	let-7a	DSN	1 pM to 10 nM	10 fM	[15]
PEC	DNA	HCR	10 fM to 10 nM	9 fM	[18]
SPR	DNA	strand displacement reaction	1 pM to 150 nM	48 fM	[13]
SWV	miRNA-21	DSN	10 fM to 1 nM	2.9 fM	This work

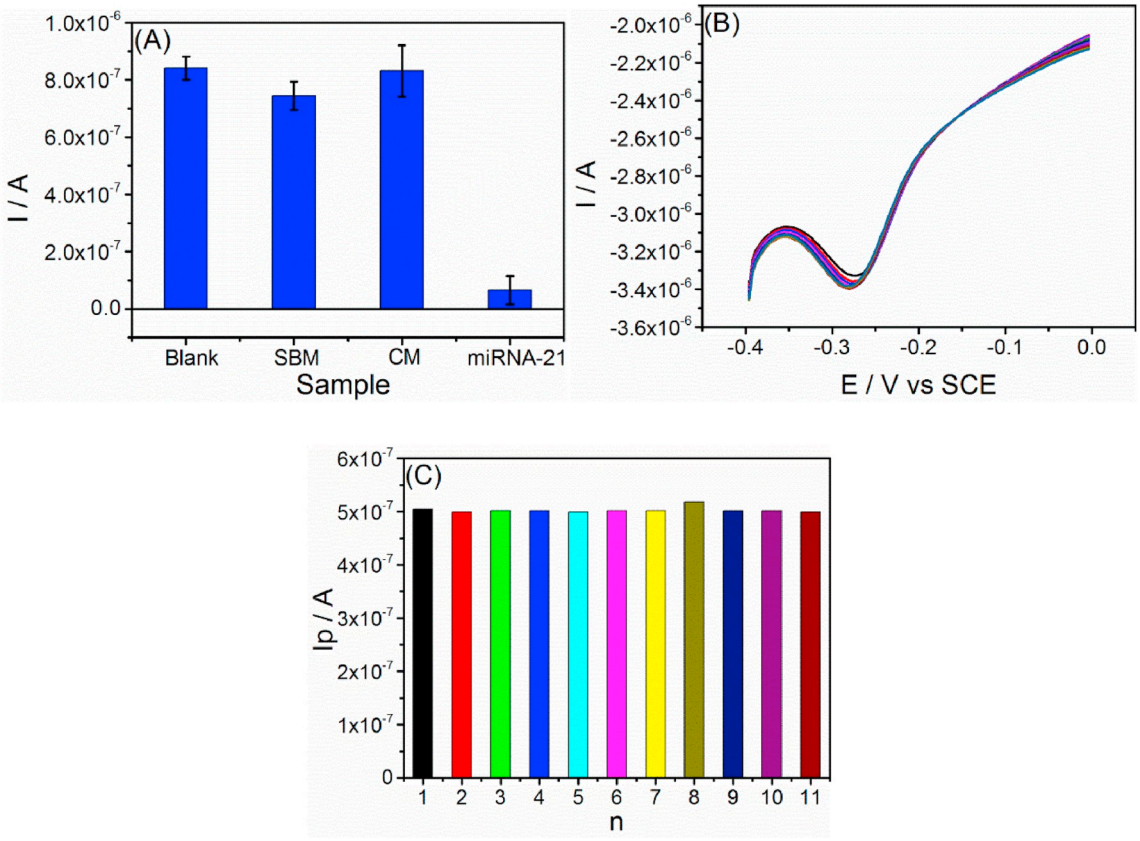

Fig. 7. (A) SWV responses of the developed biosensor in specificity for the blank, SBM, CM and miRNA-21 (B) SWV of different scan times and (C) the Ip value of different scan times.

3.6. Stability, selectivity and reproducibility of the miRNA biosensor

To investigate the selectivity of the biosensor, single base mismatch (SBM) and completely mismatched (CM) RNA sequence were utilized to replace miRNA-21 fabricated the biosensor under the optical conditions. As shown in Fig. S5 and Fig. 7A, the SWV signal of SBM and CM were higher than miRNA-21 remarkably indicating the DSN had no effective work on the mismatched RNA for the hairpin cDNA could be selectively opened by miRNA-21. Therefore, the presented electrochemical biosensor is highly specific for the detection of miRNA-21. In addition, the stability of the developed biosensor was investigated as well. From Fig. 7B and C the SWV was conducted 11 times and the signal had almost no offset. Comparing with the similar structure substrate of AuNPs/graphene, AuNPs/CNNS nanocomposite could be more stable for the electrostatic interaction of AuNPs/CNNS and affinity of Au–N [50]. The relative standard deviation (RSD) for the 11 measurements with the same biosensor under optical conditions is 1.08%. Furthermore, the RSD for five parallel measurements utilizing five biosensors constructed with the same process is 4.72% (Fig. S4), which indicates that the proposed biosensor has good stability and reproducibility.

3.7. Application of the proposed biosensor in the detection of miRNA in real samples

The standard addition method was utilized to investigate the applicability of the developed biosensor. Different concentrations of miRNA-21 were added to the human serum, and the results of the analysis were shown in Table S2. It is clearly shown that the recovery of the detection is between 94% and 104% and the RSD is below 4.57%, which suggest that the developed electrochemical biosensor has great prospect in the analysis and detection of real biological samples.

4. Conclusion

In summary, a highly sensitive and specific electrochemical biosensor has been designed for the detection of miRNAs based on AuNPs/CNNS nanocomposite and DSN assisted enzymatic target recycling method. With the electrostatic adsorption interaction of AuNPs/CNNS and affinity of Au–N, a stable substrate was constructed. Owing to the high effective of DSN and hairpin cDNA, the proposed biosensor demonstrated excellent performance with high selectivity and sensitivity. The LOD was as low as 2.9 fM. Furthermore, the biosensor has good selectivity and reproducibility for detection of miRNAs in a real sample. Therefore, the developed biosensor has a good application prospect.

Acknowledgement

This investigation was financially supported by the National Nature Science Foundations of China (No. 81571812) and A Project Funded by the Priority Academic Program Development of Jiangsu Higher Education Institutions (1107047002).

Appendix A. Supplementary data

Supplementary data to this article can be found online at https://doi.org/10.1016/j.talanta.2019.120441.

References

[1] D.P. Bartel, MicroRNAs: genomics, biogenesis, mechanism, and function, Cell 116 (2004) 281–297.
[2] H. Dong, J. Lei, L. Ding, Y. Wen, H. Ju, X. Zhang, MicroRNA: function, detection, and bioanalysis, Chem. Rev. 113 (2013) 6207–6233.
[3] L.F.R. Gebert, I.J. MacRae, Regulation of microRNA function in animals, Nat. Rev. Mol. Cell Biol. 20 (2019) 21–37.
[4] B.D. Adams, A.L. Kasinski, F.J. Slack, Aberrant regulation and function of microRNAs in cancer, Curr. Biol. 24 (2014) R762–R776.
[5] R. Subramani, L. Gangwani, S.B. Nandy, A. Arumugam, M. Chattopadhyay, R. Lakshmanaswamy, Emerging roles of microRNAs in pancreatic cancer diagnosis, therapy and prognosis (review), Int. J. Oncol. 47 (2015) 1203–1210.
[6] L. He, G.J. Hannon, MicroRNAs: small RNAs with a big role in gene regulation, Nat. Rev. Genet. 5 (2004) 522–531.
[7] R. Duan, X. Zuo, S. Wang, X. Quan, D. Chen, Z. Chen, L. Jiang, C. Fan, F. Xia, Lab in a tube: ultrasensitive detection of MicroRNAs at the single-cell level and in breast cancer patients using quadratic isothermal amplification, J. Am. Chem. Soc. 135 (2013) 4604–4607.
[8] L. Juan, Y. Bo, H. Huang, W. Zhao, S. Changhong, F. Yu, C. Qing, L. Shaolu, W. Xiang, X. Jianzhong, Real-time polymerase chain reaction microRNA detection based on enzymatic stem-loop probes ligation, Anal. Chem. 81 (2009) 5446–5451.
[9] V. Eva, B. József, H. Zoltán, MicroRNA detection by northern blotting using locked nucleic acid probes, Nat. Protoc. 3 (2008) 190–196.
[10] W. Li, K. Ruan, MicroRNA detection by microarray, Anal. Bioanal. Chem. 394 (2009) 1117–1124.
[11] S. Liu, N. Xu, C. Tan, W. Fang, Y. Tan, Y. Jiang, A sensitive colorimetric aptasensor based on trivalent peroxidase-mimic DNAzyme and magnetic nanoparticles, Anal. Chim. Acta 1018 (2018) 86–93.
[12] H. Ammari, Y. Deng, P. Millien, Surface plasmon resonance of nanoparticles and applications in imaging, Arch. Ration. Mech. Anal. 220 (2016) 109–153.
[13] W. Diao, M. Tang, S. Ding, X. Li, W. Cheng, F. Mo, X. Yan, H. Ma, Y. Yan, Highly sensitive surface plasmon resonance biosensor for the detection of HIV-related DNA based on dynamic and structural DNA nanodevices, Biosens. Bioelectron. 100 (2017) 228–234.
[14] B.Z. Chi, R.P. Liang, W.B. Qiu, Y.H. Yuan, J.D. Qiu, Direct fluorescence detection of microRNA based on enzymatically engineered primer extension poly-thymine (EPEPT) reaction using copper nanoparticles as nano-dye, Biosens. Bioelectron. 87 (2017) 216–221.
[15] M. Xiao, T. Man, C. Zhu, H. Pei, J. Shi, L. Li, X. Qu, X. Shen, J. Li, A MoS_2 nanoprobe for microRNAs quantification based on duplex-specific nuclease signal amplification, ACS Appl. Mater. Interfaces 10 (2018) 7852–7858.
[16] Y. Zhao, X. Yang, D. Han, H. Qi, Q. Gao, C. Zhang, Cyclometalated iridium-complex-based label-free supersandwich electrogenerated chemiluminescence biosensor for the detection of micro-RNA, Chemelectrochem 4 (2017) 1775–1782.
[17] H. Nan, D. Pan-Pan, Y. Tao, X. Jing-Juan, C. Hong-Yuan, A dual target-recycling amplification strategy for sensitive detection of microRNAs based on duplex-specific nuclease and catalytic hairpin assembly, Chem. Commun. 51 (2015) 13504–13507.
[18] C. Li, H. Wang, J. Shen, B. Tang, Cyclometalated iridium complex-based label-free photoelectrochemical biosensor for DNA detection by hybridization chain reaction amplification, Anal. Chem. 87 (2015) 4283–4291.
[19] M. Liang, M. Pan, J. Hu, F. Wang, X. Liu, Electrochemical biosensor for MicroRNA detection based on cascade hybridization chain reaction, Chemelectrochem 5 (2018) 1380–1386.
[20] X. Zhang, N. Bao, X. Luo, S.N. Ding, Patchy gold coated Fe3O4 nanospheres with enhanced catalytic activity applied for paper-based bipolar electrode-electrochemiluminescence aptasensors, Biosens. Bioelectron. 114 (2018) 44–51.
[21] J. Lei, H. Ju, Signal amplification using functional nanomaterials for biosensing, Chem. Soc. Rev. 41 (2012) 2122–2134.
[22] X. Gao, X. Wang, Y. Li, J. He, H.-Z. Yu, Exonuclease I-hydrolysis assisted electrochemical quantitation of surface-immobilized DNA hairpins and improved HIV-1 gene detection, Anal. Chem. 90 (2018) 8147–8153.
[23] M. Hong, M. Wang, J. Wang, X. Xu, Z. Lin, Ultrasensitive and selective electrochemical biosensor for detection of mercury (II) ions by nicking endonuclease-assisted target recycling and hybridization chain reaction signal amplification, Biosens. Bioelectron. 94 (2017) 19–23.
[24] T.T. Nguyen, B.H. The, S.Y. Hwang, N.V. Minh, Q.T. Pham, N.N. Ngoc, A. Kirtland, Y.I. Lee, Preparing cuprous oxide nanomaterials by electrochemical method for non-enzymatic glucose biosensor, Nanotechnology 29 (2018) 205501.
[25] J. Wu, X. Wang, Q. Wang, Z. Lou, S. Li, Y. Zhu, L. Qin, H. Wei, Nanomaterials with enzyme-like characteristics (nanozymes): next-generation artificial enzymes (II), Chem. Soc. Rev. 48 (2019) 1004–1076.
[26] H. Yin, Y. Zhou, H. Zhang, X. Meng, S. Ai, Electrochemical determination of microrna-21 based on graphene, LNA integrated molecular beacon, AuNPs and biotin multifunctional bio bar codes and enzymatic assay system, Biosens. Bioelectron. 33 (2012) 247–253.
[27] M. Azimzadeh, M. Rahaie, N. Nasirizadeh, K. Ashtari, H. Naderi-Manesh, An electrochemical nanobiosensor for plasma mirna-155, based on graphene oxide and gold nanorod, for early detection of breast cancer, Biosens. Bioelectron. 77 (2016) 99–106.
[28] Z. Tong, D. Yang, Z. Li, Y. Nan, F. Ding, Y. Shen, Z. Jiang, Thylakoid-inspired multishell g-C_3N_4 nanocapsules with enhanced visible-light harvesting and electron transfer properties for high-efficiency photocatalysis, ACS Nano 11 (2017) 1103–1112.
[29] H. Chen, Y.S. Rim, I.C. Wang, C. Li, B. Zhu, M. Sun, M.S. Goorsky, X. He, Y. Yang, Quasi-two-dimensional metal oxide semiconductors based ultrasensitive potentiometric biosensors, ACS Nano 11 (2017) 4710–4718.
[30] G. Presnova, D. Presnov, V. Krupenin, V. Grigorenko, A. Trifonov, I. Andreeva, O. Ignatenko, A. Egorov, M. Rubtsova, Biosensor based on a silicon nanowire field-effect transistor functionalized by gold nanoparticles for the highly sensitive determination of prostate specific antigen, Biosens. Bioelectron. 88 (2017) 283–289.
[31] H. Yin, Y. Zhou, B. Li, X. Li, Z. Yang, S. Ai, X. Zhang, Photoelectrochemical immunosensor for microRNA detection based on gold nanoparticles-functionalized g-C3N4 and anti-DNA:RNA antibody, Sens. Actuators B Chem. 222 (2016)

1119–1126.
[32] W.J. Ong, L.L. Tan, Y.H. Ng, S.T. Yong, S.P. Chai, Graphitic carbon nitride ($g\text{-}C_3N_4$)-based photocatalysts for artificial photosynthesis and environmental remediation: are we a step closer to achieving sustainability? Chem. Rev. 116 (2016) 7159–7329.
[33] E. Boisselier, D. Astruc, Gold nanoparticles in nanomedicine: preparations, imaging, diagnostics, therapies and toxicity, Chem. Soc. Rev. 38 (2009) 1759–1782.
[34] N. Li, P. Zhao, D. Astruc, Anisotropic gold nanoparticles: synthesis, properties, applications, and toxicity, Angew. Chem. Int. Ed. 53 (2014) 1756–1789.
[35] H. Jans, Q. Huo, Gold nanoparticle-enabled biological and chemical detection and analysis, Chem. Soc. Rev. 41 (2012) 2849–2866.
[36] X.-B. Qian, W. Peng, J.-H. Huang, Fluorescein-sensitized $Au/g\text{-}C_3N_4$ nanocomposite for enhanced photocatalytic hydrogen evolution under visible light, Mater. Res. Bull. 102 (2018) 362–368.
[37] S. Feng, X. Wei, L. Zhong, J. Li, A novel molecularly imprinted photoelectrochemical sensor based on $g\text{-}C_3N_4$-aunps for the highly sensitive and selective detection of triclosan, Electroanalysis 30 (2018) 320–327.
[38] B.C. Yin, Y.Q. Liu, B.C. Ye, One-step, multiplexed fluorescence detection of microRNAs based on duplex-specific nuclease signal amplification, J. Am. Chem. Soc. 134 (2012) 5064–5067.
[39] L. Xiaoyan, Z. Cheng, H. Yishun, Z. Zhi, C. Xi, Y. Chaoyong James, Backbone-modified molecular beacons for highly sensitive and selective detection of microRNAs based on Duplex specific nuclease signal amplification, Chem. Commun. 49 (2013) 7243–7345.
[40] R. Zhong, Q. Tang, S. Wang, H. Zhang, F. Zhang, M. Xiao, T. Man, X. Qu, L. Li, W. Zhang, Self-assembly of enzyme-like nanofibrous G-molecular hydrogel for printed flexible electrochemical sensors, Adv. Mater. 30 (2018) 1706887.
[41] Z. Zhou, Q. Shang, Y. Shen, L. Zhang, Y. Zhang, Y. Lv, Y. Li, S. Liu, Y. Zhang, Chemically modulated carbon nitride nanosheets for highly selective electrochemiluminescent detection of multiple metal-ions, Anal. Chem. 88 (2016) 6004–6010.
[42] K. Kwan, L. Hyang Bong, L.J. Won, P. Hyoung Kun, S. Kuan Soo, Self-assembly of poly(ethylenimine)-capped Au nanoparticles at a toluene-water interface for efficient surface-enhanced Raman scattering, Langmuir the ACS Journal of Surfaces & Colloids 24 (2008) 7178–7183.
[43] Z. Xiaodong, X. Xiao, W. Hui, Z. Jiajia, P. Bicai, X. Yi, Enhanced photoresponsive ultrathin graphitic-phase C_3N_4 nanosheets for bioimaging, J. Am. Chem. Soc. 135 (2013) 18–21.
[44] W.-J. Song, J.-Z. Du, T.-M. Sun, P.-Z. Zhang, J. Wang, Gold nanoparticles capped with polyethyleneimine for enhanced siRNA delivery, Small 6 (2010) 239–246.
[45] F. Xu, H. Dong, Y. Cao, H. Lu, X. Meng, W. Dai, X. Zhang, K.A. Al-Ghanim, S. Mahboob, Ultrasensitive and multiple disease-related MicroRNA detection based on tetrahedral DNA nanostructures and duplex-specific nuclease-assisted signal amplification, ACS Appl. Mater. Interfaces 8 (2016) 33499–33505.
[46] X.-L. Huo, H. Yang, W. Zhao, J.-J. Xu, H.-Y. Chen, Nanopore-based electrochemiluminescence for detection of MicroRNAs via duplex-specific nuclease-assisted target recycling, ACS Appl. Mater. Interfaces 9 (2017) 33360–33367.
[47] N. Xia, K. Liu, Y. Zhou, Y. Li, X. Yi, Sensitive detection of microRNAs based on the conversion of colorimetric assay into electrochemical analysis with duplex-specific nuclease-assisted signal amplification, Int. J. Nanomed. 12 (2017) 5013–5022.
[48] E. Xiong, X. Zhang, Y. Liu, J. Zhou, P. Yu, X. Li, J. Chen, Ultrasensitive electrochemical detection of nucleic acids based on the dual-signaling electrochemical ratiometric method and exonuclease III-assisted target recycling amplification strategy, Anal. Chem. 87 (2015) 7291–7296.
[49] L. Zhang, X. Xiao, Y. Xu, D. Chen, J. Chen, Y. Ma, Z. Dai, X. Zou, Electrochemical assay for continuous monitoring of dynamic DNA methylation process, Biosens. Bioelectron. 100 (2018) 184–191.
[50] H. Wei, B. Li, Y. Du, S. Dong, E. Wang, Nucleobase – Metal hybrid Materials: preparation of submicrometer-scale, spherical colloidal particles of Adenine – Gold(III) via a supramolecular hierarchical self-assembly approach, Chem. Mater. 19 (2007) 2987–2993.
[51] S. Zhang, R. Liu, Z. Xing, S. Zhang, X. Zhang, Multiplex miRNA assay using lanthanide-tagged probes and duplex-specific nuclease amplification strategy, Chem. Commun. 52 (2016) 14310–14313.